dc responsivity of proximity effect bridges to high frequency radiation

M. G. Hauser, D.W. Palmer

dc RESPONSIVITY OF PROXIMITY EFFECT BRIDGES TO HIGH FREQUENCY RADIATION

M. G. HAUSER and D. W. PALMER

California Institute of Technology, Pasadena, California 91109, USA

Résumé. — L'effet d'un rayonnement hyperfréquence sur la caractéristique courant-tension de micropont à effet de proximité en niobium et en tantale a été étudié aux fréquences 10, 35 et 90 GHz.

La fraction ε de la puissance rayonnée incidente absorbée directement par le micropont est déterminée par une mesure calorimétrique, ce qui permet de connaître sa réponse intrinsèque (en volt par watt de puissance absorbée lorsqu'il est polarisé par un courant). ε est de l'ordre de 10^{-4} pour un pont Nb-Ta de 0,1 Ω et croît comme le carré de la résistance R de la jonction mesurée en courant continu.

La réponse en large bande est en général indépendante de la puissance incidente mais croît avec le courant critique I_c et décroît lorsque la fréquence augmente. Elle varie approximativement comme Ω^{-3} si Ω est la fréquence normalisée $\hbar\omega/2\,eRI_c$.

Les meilleures réponses obtenues actuellement sont de 10^5 V/W absorbé à 10 GHz et 10^2 V/W absorbé à 90 GHz.

En plaçant les jonctions dans le vide et en les exposant à un rayonnement dans le proche infrarouge, on remarque que leur réponse thermique est bien plus faible que leur réponse aux hyperfréquences à 90 GHz.

Abstract. — The effect of microwave radiation on the dc current-voltage characteristic of proximity effect bridges has been studied at frequencies of 10, 35 and 90 GHz. We report the properties of bridges fabricated in layered films of Nb and Ta. The fraction ε of the incident radiant power absorbed by the bridge is measured calorimetrically, permitting determination of the intrinsic responsivity (volts per watt of power absorbed when operated in a current-biased mode). In our test geometry ε is typically $\sim 10^{-4}$ for a 0.1 Ω Nb-Ta bridge, and increases roughly linearly with dc junction resistance R. Broad-band responsivity is generally independent of incident power. increases with increasing critical current I_c (decreasing temperature), and decreases with increasing frequency, varying approximately as Ω^{-3} where Ω is the normalized frequency $\hbar\omega/2\,eRI_c$. Peak responsivities achieved to date are $\sim 10^5$ V/W (absorbed) at 10 GHz and $\sim 10^2$ V/W (absorbed) at 90 GHz. By mounting junctions in vacuum and exposing them to near-infrared radiation, we have found that their purely bolometric (thermal) response is much weaker than the microwave response at 90 GHz.

1. **Introduction.** — In the preceding paper, Mercereau has discussed the properties of proximity effect microbridges fabricated in multilayered thin films of hard superconductors. Because these rugged and stable structures are physically well-suited to incorporation in practical devices, we have undertaken to explore and develop their capabilities as detectors for millimeter and submillimeter radiation. Our particular interest is in new detectors for astronomical observations in the 0.3-3 mm wavelength range.

We report here the results of video mode responsivity measurements made with coherent sources at 10, 35 and 90 GHz, and of an investigation of the thermal response to incoherent near-infrared radiation. These studies were designed primarily to compare the responsivities of bridges of different materials, geometries and electrical characteristics, and to determine the frequency dependence of the responsivity in the millimeter wavelength range. To pursue these objectives efficiently, the test geometry and instrumentation have been kept quite simple ; it has not been necessary either to optimize the coupling to incident radiation or to minimize noise in the measuring instruments. The results, however, allow one to estimate the ultimate sensitivity of presently available devices for detection of millimeter and submillimeter radiation, and suggest ways in which these devices should be modified for improved high-frequency performance.

2. **Physical characteristics of the proximity effect bridge.** — The bridges we have studied are fabricated in multilayered films of hard superconductors such as Nb, Ta, Zr and W. Photoresist and anodization techniques are used to produce microstructure in the films. These techniques have been described briefly by Notarys and Mercereau [1] and in detail by Palmer and Decker [2]. Figure 1 shows schematically the structure of such a bridge in a two-layer film, the upper film having a higher critical temperature T_c

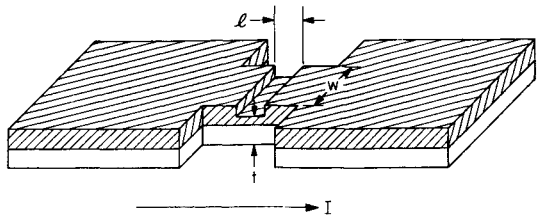

FIG. 1. — Schematic of a proximity effect junction in a two-layer film structure. The material of the upper film has a higher critical temperature than that of the lower one. The arrow indicates the direction of bias current flow.

than the lower film. The dimensions l, w and t are the length, width and thickness, respectively of the bridge region. The films are usually evaporated onto sapphire slides. The critical temperature of the bridge region is lower than that in the remainder of the film for two reasons : (*a*) T_c in a single layer decreases as its thickness is reduced ; (*b*) proximity of the low T_c material to the high T_c material lowers T_c for the entire film, and lowers it most in the bridge region where the high T_c material is thinnest.

Table I lists some of the material and thickness combinations which we have tried. We find that the critical temperature of the weakened region in Nb-Ta films is less sensitive to the depth of anodization than with the other materials, making it easier to fabricate Nb-Ta bridges with predictable electrical characteristics. The Nb-Ta films also show radiation responsivity at least as good as that of the other combinations tested. For these reasons, we shall present here only results obtained with Nb-Ta films.

TABLE I

Summary of multilayer films

Materials	Thicknesses (Å)			
Nb	100	125	200	200
Ta	200	200	200	300
Nb	100			
Zr	200			
Nb	100			
Ta	100			
Zr	100			
W	175	263	350	
Ta	350	350	350	

The properties of the particular bridges included in this report are summarized in table II. These bridges are all appreciably shorter than 1 μ. The high frequency response of proximity effect bridges generally improves as l is decreased, at least to the present limit of our fabrication methods of about 0.3 μ. For example, there is very little response to 10 GHz radiation for bridges longer than 1.5 μ, whereas bridges with l in the range 0.3-0.5 μ show strong 10 GHz response. The width plays a role in high frequency response primarily through its effect on the differential resistance R. All else being equal, large R is desirable for good radiation coupling efficiency (section 3.2) and high responsivity (section 3.4). However, for our typical film thickness of 100-200 Å per layer, the bridge must be at least 5 μ wide to minimize the likelihood of electrical burn-out. There is some indication that films thicker than 300 Å would give more responsive bridges, but our present anodization techniques do not permit structuring on a 0.3 μ scale in thicker films.

3. **Coherent source tests.** — 3.1 APPARATUS AND METHODS. — Responsivity measurements at 10, 35 and 90 GHz are made using klystrons as radiation sources. The film containing the junction is mounted transversely close to the end of a section of rectangular waveguide which is immersed in a He bath. The bridge is oriented so that the electric field of the fundamental waveguide mode is parallel to the direction of flow of the bias current. A simplified schematic of the apparatus is shown in figure 2. The junctions are current-biased, with provisions for three types of measurement : (1) the differential resistance dV/dI can be measured by adding a small ac component to the bias current I ; (2) the voltage responsivity can be measured by chopping the microwave radiation ; and (3) the V-I curve can be observed directly by chopping the full bias current (chopper not shown in figure 2). In all three modes of operation the junction voltage is measured using phase sensitive detection and recorded as a function of bias current. Chopping of the radiation at about a 1 kHz rate is accomplished with a pin diode modulator at 10 GHz and with klystron modulation at 35 and 90 GHz.

TABLE II

Properties of the Nb-Ta *bridges included in this report*

Designation	Film thickness (Å)		Bridge dimensions			R (Ω)
	Nb	Ta	l (μ)	w (μ)	t (Å)	
D-3(1)	130	216	0.3-0.4	7	246	0.1
TBS 9a	100	240	0.35	20	180	0.04
CIT 11a(1A)	200	240	0.4-0.6	26	140	0.1
CIT 12a(5A)	115	184	0.4-0.5	20	100	0.025

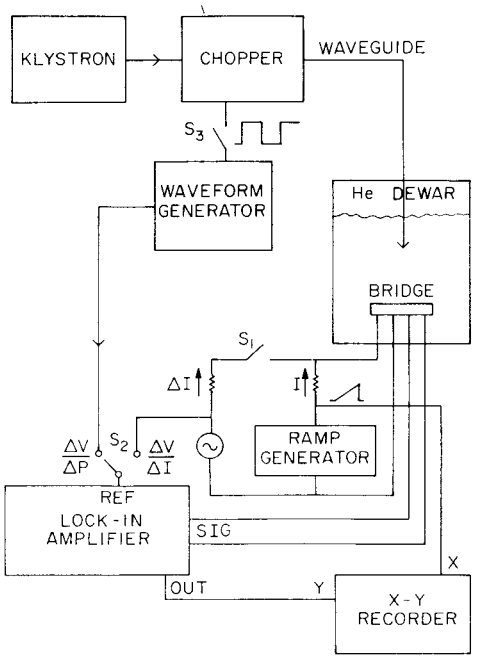

FIG. 2. — Schematic of apparatus for coherent source tests. The switches may be set to observe either the $\frac{dV}{dI}$-I characteristic (modulated bias current) or the voltage responsivity (modulated radiation) as a function of bias current.

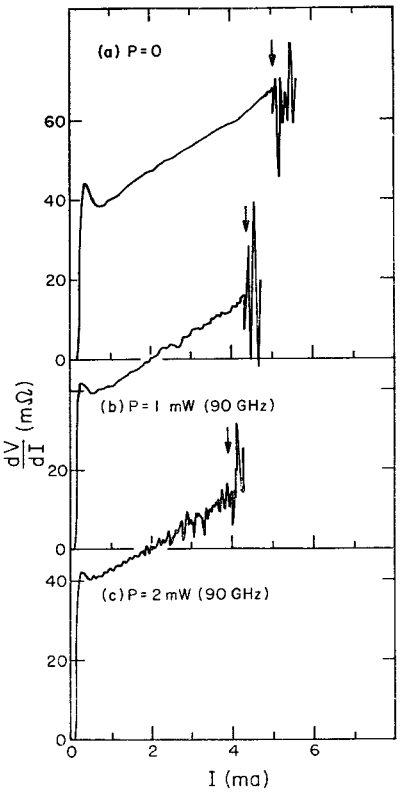

FIG. 3. — Differential resistance characteristics of junction TBS 9a showing the noise associated with localized boiling in the He bath. Curves (*a*), (*b*) and (*c*) correspond to incident 90 GHz power levels of 0, 1 and 2 mW respectively.

3.2 RADIATION COUPLING EFFICIENCY. — In order to determine the intrinsic responsivity of each bridge, that is, the response per unit of radiant power absorbed by the junction, it is necessary to know the fraction ε of incident power being absorbed by the bridge. We find that the amount of radiant power dissipated in the bridge can be measured with modest accuracy using the dc substitution method illustrated in figure 3. This figure shows dV/dI curves for three different microwave power levels. In each case the curve becomes markedly noisier when the power dissipated in the bridge is sufficient to cause locally active boiling in the He bath. The dc power required for boiling decreases linearly with increasing rf power. The change in dc power is therefore taken as the amount of rf being absorbed. It should be noted that the amplitude of the « boiling noise » on the dV/dI curve is not usually as large as shown in figure 3, but even a small increase in noise at a well-defined bias current is readily discernible. Measurements of ε made on a single bridge in the different test assemblies for 10, 35 and 90 GHz are generally in agreement.

Simple impedance matching considerations suggest that ε should depend linearly on the junction resistance R. It is difficult to verify this behavior over any substantial resistance range because some other junction parameter, such as length, width, or thickness, must be changed in order to change R, and ε appears to depend to some extent on all of them. In our test geometry we find that bridges with $R \sim 0.1\ \Omega$ have ε in the range 10^{-4} to 10^{-3}, whereas those with $R \sim 1\ \Omega$ have $\varepsilon \sim 10^{-2}$.

3.3 EFFECTS OF RADIATION ON THE I-V CHARACTERISTIC. — High frequency radiation modifies the dc current-voltage characteristic of a proximity effect bridge in much the same way as other Josephson-effect devices : the current amplitude I_0 of the zero-voltage step is modified, and additional constant-voltage steps appear in the V-I curve [1]. Figures 4*a* and 4*b* illustrate the effect of 90 GHz power on bridge CIT 11a(1A). These data show the appearance of harmonic steps at $V = n\hbar\omega/2$ e with $n = 1$ and 2 and subharmonic steps at $n = 1/5$, $1/4$, $1/3$ and $1/2$, as well as a decrease in I_0 with increasing rf power. The highest harmonic step observed with 90 GHz radiation is $n = 2$, this limit being set at least in part by power limitations of our 90 GHz source and by a tendency of the films to become normal at the bias currents required to reach higher steps. We have observed steps to $n \sim 27$ with 10 GHz radiation.

We have been particularly interested in testing the frequency dependence of the effect of radiation on I_0, since the modulation of I_0 is the basis for broad band video detection with these devices. The rf voltage source model for a voltage-biased tunnel junction predicts [3] that

$$\frac{I_0}{I_c} = J_0\left(\frac{2eV_r}{\hbar\omega}\right), \qquad (1)$$

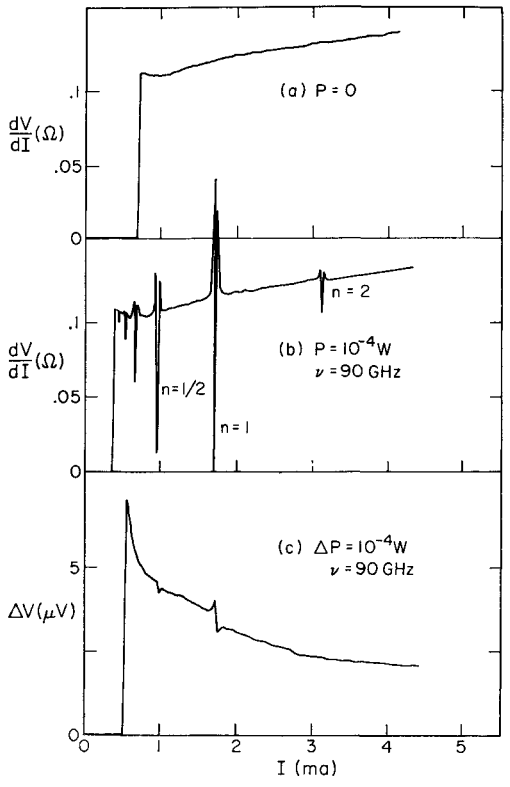

FIG. 4. — Differential resistance and voltage responsivity as a function of dc bias current for bridge CIT 11a(1A) at 4.19 K. (*a*) dV/dI with no microwave power incident, (*b*) dV/dI with 10^{-4} W of continuous 90 GHz power. The features correspond to steps in the V-I curve at voltages $V = n\hbar\omega/2\ e$ (*c*) voltage response to 10^{-4} W (peak) of chopped 90 GHz power.

where I_c is the critical current with no rf, J_0 is the Bessel function of order zero, and V_r is the rf voltage induced by the radiation. Russer [4] has made analog computer calculations of the effect of large rf signals on the current-driven, resistively shunted junction. He found that the Bessel function behavior of eq. (1) still holds provided that the normalized frequency Ω, defined by

$$\Omega = \frac{\hbar\omega}{2\,eI_c\,R} \tag{2}$$

is greater than unity, but that I_0 decreases more rapidly with increasing power for $\Omega < 1$. Though the relation between supercurrent and voltage in a proximity effect junction is not the same as that of a tunnel junction [1], the equation governing the time-dependence of the voltage of a current-biased, current-driven proximity effect junction is of the same form as that studied by Russer. We therefore expect similar behavior for our bridges.

The variation of I_0 with radiant power in the large signal regime is summarized for several Nb-Ta proximity effect bridges in figure 5. Here we show the ratio I_0/I_c as a function of the rf signal normalized to the voltage at the first rf induced step

$$x = \frac{2\,e}{\hbar\omega}(\varepsilon PR)^{1/2}, \tag{3}$$

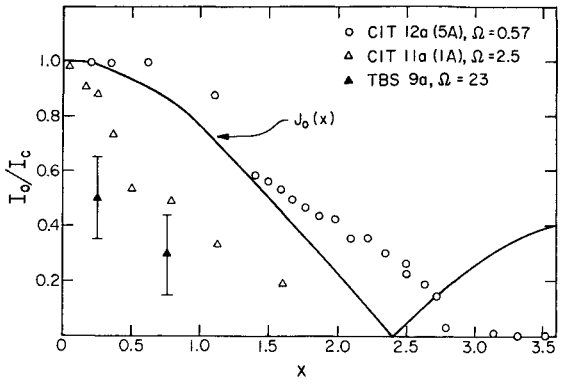

FIG. 5. — Current amplitude of the zero voltage step as a function of the normalized rf signal x (see eq. (3)) for several Nb-Ta bridges. Circles and triangles are data obtained with 10 and 90 GHz radiation respectively. The normalized frequency $\Omega = \hbar\omega/2\,eI_c\,R$ is indicated for each bridge.

where P is the incident power. If one supposes that absorbed power is related to V_r by

$$\varepsilon P = \frac{V_r^2}{R}, \tag{4}$$

then x is also the argument of the Bessel function in eq. (1). The circles and triangles in figure 5 are data obtained with 10 and 90 GHz radiation respectively. In all cases the coupling efficiency ε was determined from the « boiling » analysis discussed in section 3.2, with an estimated uncertainty of a factor of 2. Bearing in mind that the uncertainty in ε introduces a 40 % uncertainty in the abscissa for each independent set of points in figure 5, these data are roughly consistent with the smooth curve representing the Bessel function of eq. (1). This observation suggests the following conclusions : (1) for $\Omega \gtrsim 1$, the size of the zero-voltage step for the proximity effect bridges varies according to eq. (1) ; (2) as an alternative to the boiling analysis (section 3.2), ε can be determined from the power dependence of I_0, for example, from

$$\varepsilon = 2.4\left(\frac{\hbar\omega}{2\,e}\right)^2 (P_0\,R)^{-1}, \tag{5}$$

where P_0 is the incident power at angular frequency ω which drives I_0 to zero ; (3) the relation between absorbed power and rf signal is represented reasonably well by eq. (4) ; and (4) the power required to produce a given modulation of the critical current is proportional to the square of the radiation frequency.

The last of these conclusions is somewhat in conflict with our measurements of the response to small rf signals, as discussed in section 3.4.4 below.

3.4 VIDEO MODE RESPONSIVITY. — 3.4.1 *Definition of the responsivity.* — Figure 4*c* shows the voltage response of a Nb-Ta bridge to chopped 90 GHz radiation. The response is strongest at a bias current

slightly greater than the critical current and shows features corresponding to the $n = \frac{1}{2}$ and $n = 1$ steps in the *V-I* curve. We shall restrict our attention to the intrinsic responsivity r measured for bias current I slightly larger than the critical current and examine its dependence on incident power, critical current and frequency. Intrinsic responsivity is defined as the peak-to-peak variation in dc junction voltage divided by the peak absorbed rf power.

A junction current-biased with $I \gtrsim I_0$ will respond to chopped radiation with a voltage change dependent upon the modulation of I_0 and on the differential resistance at the bias point. For small signals, under the assumption that the voltage change is proportional to the change in I_0, eq. (1) predicts a response in this mode proportional to the power and inversely proportional to ω^2. Kanter and Vernon [5] have used a perturbation technique to solve the equation for a current-biased junction shunted by a normal conductance in the presence of radiation, and for small signals find the voltage response

$$\Delta V = \frac{1}{4} \frac{I_r^2 R}{I \Omega^2} \qquad (6)$$

in the limit $(2\,eV/\hbar\omega) \ll 1$, where I_r is the rf current. This response is proportional to the power, inversely proportional to ω^2, and proportional to I_c^2. In the preceding paper, Mercereau shows that similar behavior is expected for proximity effect bridges.

3.4.2 *Power dependence.* — Since the junction response in this detection mode is expected to be proportional to the signal power for small signals, we expect the responsivity to be independent of power. We find this to be the case over a considerable range of incident power, as illustrated in figure 6 for 90 GHz signals. The normalized rf signal x (eq. (3)) is much less than unity for these data. Similar results are found at the lower frequencies at low power levels. Thus, we can reasonably characterize the junction response to small signals by a well-defined responsivity.

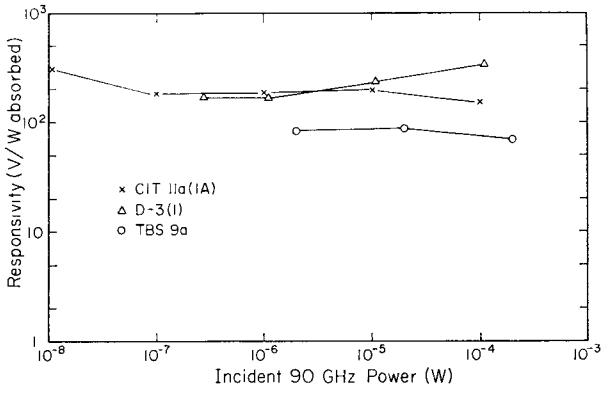

FIG. 6. — Intrinsic responsivity achieved at 90 GHz with several Nb-Ta bridges as a function of incident power. The bias current and temperature for each bridge were fixed at the values giving maximum response.

3.4.3 *Critical current dependence.* — An important parameter affecting junction response is the critical current I_c. Kirschman studied the ac response of proximity effect bridges in the frequency range 10-450 MHz, and concluded that the response can be characterized rather completely in terms of I_c and the resistance R [6]. The critical current of these structures is a sensitive function both of temperature T and static magnetic field as well as incident rf power level [1]. Kirschman varied I_c over a wide range by applying a magnetic field and by applying high frequency radiation. He found (for large signals) that the normalized ac signal (essentially the parameter x of eq. (3)) required to maximize the amplitude of the $n = 1$ step is a function only of the normalized frequency Ω (eq. (2)), regardless of the conditions used to achieve a given critical current.

We have not duplicated Kirschman's experiment at high frequency, though we have observed that suppression of I_c with magnetic field certainly suppresses the response. We normally adjusted the external magnetic field to maximize I_c. We have explored the dependence of r on I_c by varying T. Here the result is not quite so simple, for we find different behavior depending upon whether T is high (within $\sim$ 0.3 K of the transition temperature of the bridge) or low. As T decreases below the transition temperature, I_c first shows the rapid exponential rise characteristic of weakly-coupled superconductors, then continues to rise much more slowly as expected for strongly-coupled superconductors [1]. The responsivity shows different dependence on I_c in these two temperature ranges. Figure 7 shows

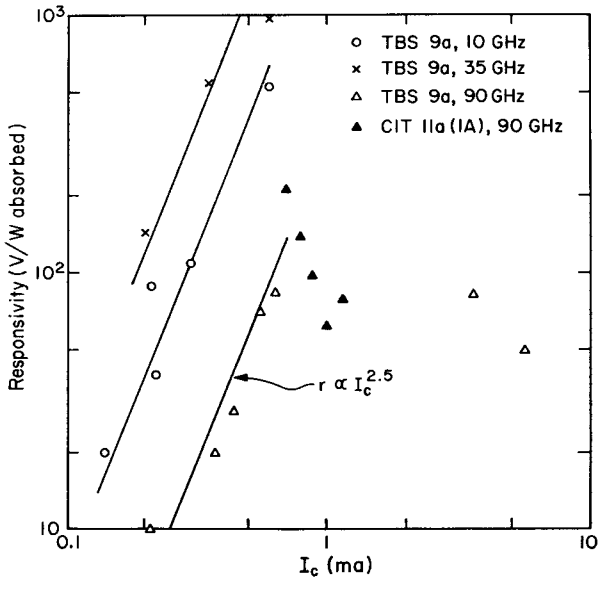

FIG. 7. — Dependence of responsivity on critical current. The responsivity scale should be multiplied by 10^2 for the 10 GHz data. For each bridge the critical current was raised by lowering the temperature. The TBS 9a data above 1 ma and CIT 11a(1A) data were obtained at temperatures well below the transition temperature, whereas the remaining data were obtained close to the transition temperature.

the 90 GHz responsivity as a function of critical current for two Nb-Ta bridges. The TBS 9a data for $I_c < 1$ ma were obtained by varying T over a 0.2 K interval close to 4.2 K, where I_c shows a rapid exponential variation with T. In this range the responsivity varies strongly with I_c, increasing roughly as $I_c^{2.5}$. However, for $T \approx 3$ K, where I_c is close to 4 ma and increases slowly with decreasing T, the responsivity is no greater than at 0.6 ma and is decreasing with further increase in I_c. The data for bridge CIT 11a(1A) were also obtained well below the transition temperature and show a similar decrease in responsivity with increasing I_c.

These results indicate that for a range of temperatures extending some distance below the bridge transition temperature, the critical current does characterize the junction response to radiation, with responsivity varying nearly quadratically with I_c as predicted by the current-biased junction model (see eq. (6)). At low temperature, however, this behavior breaks down and the junction becomes a less sensitive radiation detector. In the high temperature range, the rapid variation of responsivity with I_c and the strong dependence of I_c on T imply that good temperature regulation will be needed for stable detector operation.

3.4.4 *Frequency dependence.* — The variation of small-signal responsivity with radiation frequency over the 10-90 GHz range is shown in figure 8. The data in figure 8 are consistent with

$$r \propto \omega^{-3}, \qquad (7)$$

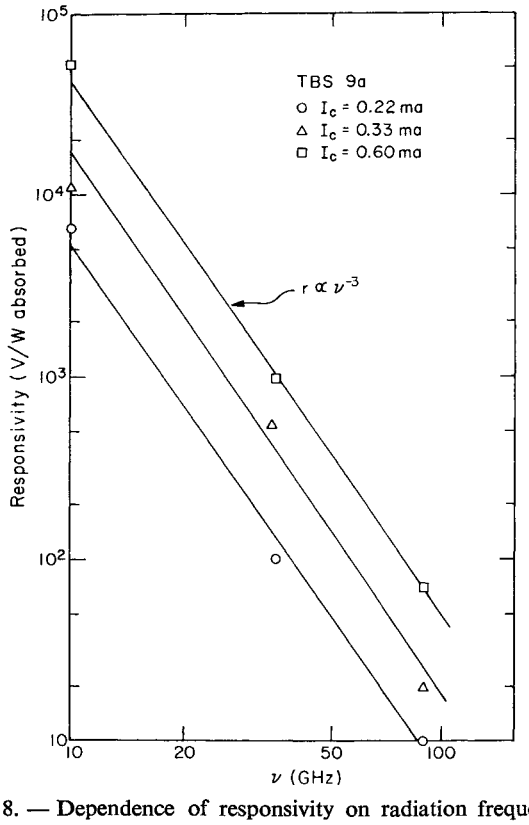

FIG. 8. — Dependence of responsivity on radiation frequency for several values of the critical current I_c.

which is a more rapid decrease with increasing frequency than the ω^{-2} dependence predicted by eq. (6) or suggested by the large-signal data in figure 5. The largest relative uncertainty in the data at different frequencies lies in the determination of the absorbed power. While the boiling analysis (section 3.2) has considerable uncertainty, we consider it unlikely that the exponent in eq. (7) is in error by more than 10 %. Note that the apparent discrepancy in the frequency dependence suggested by our large-signal and small-signal measurements cannot be explained in terms of an error in the radiation coupling efficiency, since both analyses use the same values of ε. Though we cannot explain this discrepancy, if indeed it is real, our conclusions are not greatly affected by it, for extrapolation of the responsivity to frequencies appreciably above the measured range is in any case highly unreliable. We examine the implications of the responsivity measured at 90 GHz in section 3.5 below.

It is interesting to display explicitly the relation between responsivity and the normalized frequency Ω. The data for bridge TBS 9a are most extensive and are shown in figure 9. At each frequency the critical current was varied by changing the temperature, and at each T the magnetic field was adjusted for maximum I_c. All points except the 90 GHz measure-

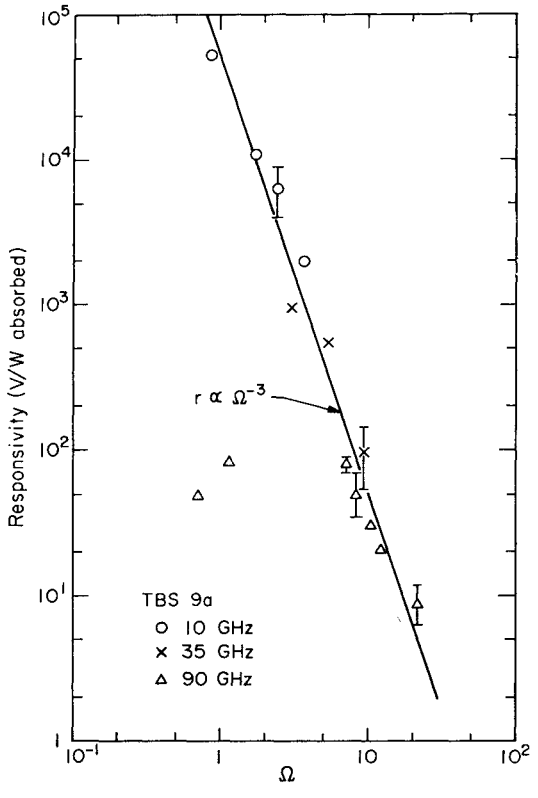

FIG. 9. — Dependence of responsivity on the normalized frequency $\Omega = \hbar\omega/(2\,eI_c\,R)$ for a single proximity effect bridge. Measurements made at 10, 35 and 90 GHz are shown with different symbols. All data except the 90 GHz points at $\Omega \approx 1$ were obtained close to the bridge transition temperature.

TABLE III

Video mode sensitivity for a single proximity effect bridge

Frequency (GHz)	Responsivity (V/W absorbed)	NEP (W/Hz$^{1/2}$) Achieved	Johnson noise	$\varepsilon = 1$
10	10^5	2×10^{-11}	8×10^{-14}	6×10^{-17}
90	2×10^2	7×10^{-9}	4×10^{-11}	3×10^{-14}

ments at $\Omega \approx 1$ were obtained at temperatures close to the bridge transition temperature. For operation in this temperature range we see the strong dependence of r on Ω expected from figures 7 and 8, the data being quite consistent with $r \propto \Omega^{-3}$. More limited data obtained with other bridges support this same conclusion.

3.5 VIDEO MODE SENSITIVITY. — In the response mode examined here, an appropriate figure of merit for operation as a detector is the noise equivalent power (NEP), defined as the signal power producing unity signal-to-noise ratio in a postdetection bandwidth of 1 Hz. Because we have neither maximized the radiation coupling efficiency nor minimized the instrumental noise, the sensitivity achieved in our responsivity studies is not as high as that potentially realizable with these devices. Some representative values, based upon the responsivities we have observed at 10 and 90 GHz for single junctions, are listed in table III. The second column shows typical intrinsic responsivities of good bridges. The third column is the NEP achieved in our nonresonant test geometry with an instrumental noise level of about 10^{-9} V/Hz$^{-1/2}$. The fourth column indicates the NEP for the same responsivity and coupling efficiency if instrumental noise were reduced until limited by Johnson noise in the weak link itself. The last column is a projection of the NEP for a Johnson-noise limited bridge if highly efficient radiation coupling could be achieved.

The sensitivities shown in the last column of table III are attractive when compared with available broad-band detectors. It remains to be demonstrated, therefore, that such performance can be achieved. Kirschman and Mercereau have reported measurements of current noise in proximity effect bridges which indicate that the device noise is dominated by Johnson noise [7]. Since voltmeters capable of measuring Johnson noise in 10^{-1} Ω sources at 4 K have been developed [8], it seems likely that sensitivity close to that shown in the fourth column of table III can be achieved with no improvements in responsivity or coupling efficiency. The coupling problem appears more difficult, and we are just beginning to consider it. Preliminary tests with junctions mounted between the end of the waveguide and a reflecting plate or in resonant cavities have shown increases as large as two orders of magnitude in power absorption over that found in our open waveguide geometry. Since resonant geometry also reduces the spectral bandwidth of the detection system, a useful increase in sensitivity occurs only if the source has a correspondingly restricted spectrum. Coupling methods will therefore have to be chosen with particular applications in mind, but these initial tests offer encouraging indications that substantial gains over the coupling efficiency of our simple test geometry can be realized.

Thus, it appears that prospects are good for achieving usefully high sensitivity with our present Nb-Ta proximity effect bridges at wavelengths of a few millimeters. If experiments at frequencies above 90 GHz show the responsivity to continue to fall as rapidly as ω^{-2} or ω^{-3} (section 3.4.4), these particular bridges are unlikely to be more sensitive detectors of submillimeter radiation than currently available semiconducting bolometers. However, we noted in section 2 that high-frequency response increases as the bridge length is reduced and the film thickness is increased. We have recently been trying new fabrication techniques which promise to extend our capabilities in both of these directions and thus bring us closer to producing detectors of superior sensitivity for wavelengths extending into the submillimeter range.

4. Thermal response. — The magnitude of the thermal (bolometric) response of these proximity effect bridges is of considerable practical importance. The thermal response of the system will set a lower limit on the video mode microwave response one can detect. If the bolometric response is large, noise introduced by temperature fluctuations in the bath may predominate over Johnson noise in the junction. Finally, many millimeter wave sources and commonly encountered backgrounds have very substantial near-infrared fluxes associated with them. Small thermal response will simplify the filtering requirements for millimeter measurements on such sources.

In order to observe the thermal response, we mounted junction TBS 9a in vacuum to increase its thermal time constant, and exposed it to chopped radiation from a 10^3 K blackbody source. The source was unfiltered so that most of the incident power was at a wavelength much shorter than any expected to produce a coherent response in the junction. The sapphire slide supporting the junction was mounted on a copper block which, in turn, contacted the outside of a liquid helium reservoir. For a thermal detector the amplitude of the response and phase with respect

to the chopper phase depend upon the chopping frequency. We raised the chopping frequency from 5 to 80 Hz and found that the signal amplitude decreased and the phase shifted in the manner expected for a thermal detector with a time constant of about 10 ms.

As in the coherent source tests, the junction was current-biased and the magnetic field was adjusted for maximum critical current. The voltage signal observed per watt of *incident* power, in the limit of low chopping frequency, was a factor of 10^2 smaller than the response of the same junction to 90 GHz power. This is a lower limit on the ratio of millimeter-wave responsivity to thermal responsivity in a He bath, since the fraction of incident power being absorbed in our vacuum mounting was higher than in the microwave responsivity tests and the thermal conductance in the vacuum was smaller than in the bath. In any event, this result shows that these detectors can be operated with much better rejection of near-infrared radiation than conventional bolometers.

Acknowledgments. — We would like to acknowledge many helpful discussions with H. Notarys and J. Mercereau and the able assistance of M. Pickar in the thermal response studies. This work was supported in part by the Office of Naval Research Contract N00014-67-A-0094-0013, the Director's Fund of the Jet Propulsion Laboratory and NASA Grant NGL05-002-007.

References

[1] NOTARYS, H. A. and MERCEREAU, J. E., *J. Appl. Phys.* **44** (1973) 1821.

[2] PALMER, D. W. and DECKER, S. K., *Rev. Sci. Instrum.* (to be published).

[3] RICHARDS, P. L., AURACHER, F. and VAN DUZER, T., *Proc. IEEE* **61** (1973) 36.

[4] RUSSER, S. P., *J. Appl. Phys.* **43** (1972) 2008.

[5] KANTER, H. and VERNON, F. L., Jr., *J. Appl. Phys.* **43** (1972) 3174.

[6] KIRSCHMAN, R. K., *Low Temp. Phys.* **11** (1973) 235.

[7] KIRSCHMAN, R. K. and MERCEREAU, J. E., *Phys. Lett.* **35A** (1971) 177.

[8] CLARKE, J., *Proc. IEEE* **61** (1973) 8.